Materials Science & Engineering A 733 (2018) 153–163

Contents lists available at ScienceDirect

Materials Science & Engineering A

journal homepage: www.elsevier.com/locate/msea

The microstructures and properties changes induced by Al:Co ratios of the $Al_XCrCo_{2-X}FeNi$ high entropy alloys

Yuqiao Zhao, Hongzhi Cui*, Mingliang Wang, Yong Zhao, Xue Zhang, Canming Wang

School of Materials Science and Engineering, Shandong University of Science and Technology, Qingdao 266590, China

ARTICLE INFO

Keywords:
$Al_XCrCo_{2-X}FeNi$
High Entropy Alloy
Microstructure
Wear resistance
Mechanical property

ABSTRACT

The formation High Entropy Alloys (HEAs) from combinations of multiple principal elements, with differing molar ratios, has led to the suggestion that the properties of HEAs must be dramatically changed. In this study, a series of five-component $Al_XCrCo_{2-X}FeNi$ HEAs were prepared by using spark plasma sintering (SPS). The effect of the Al:Co ratios on the phases and microstructures of $Al_XCrCo_{2-X}FeNi$ HEAs were investigated. It was found that the microstructures changed from a Fe- and Cr-rich face-centered cubic (FCC) structure to a Ni- and Al-rich body-centered cubic (BCC) structure with an increase in the molar ratios of Al:Co; clearly different morphologies of the four HEAs were observed. The crystal structures of the $Al_XCrCo_{2-X}FeNi$ HEA evolved from FCC + σ + disordered BCC + ordered BCC structures to σ + disordered BCC + ordered BCC structures, and then to disordered BCC + ordered BCC structures. Moreover, the wear behavior and compression behavior of the samples at x = 1.0, 1.2, 1.4, and 1.6 were investigated. With an increase molar ratios of Al:Co, the series of $Al_XCrCo_{2-X}FeNi$ HEAs exhibited different wear and fracture mechanisms. The results showed that the $Al_{1.6}CrCo_{0.4}FeNi$ alloy exhibited good wear resistance, and the $Al_{1.4}CrCo_{0.6}FeNi$ alloy exhibited good combinations of strength and ductility. The close relationship between the microstructures and mechanical properties of the HEAs are discussed with a focus on balancing the strength and plasticity of the alloys for practical applications.

1. Introduction

Recently, a novel class of alloys based on the theory of high-entropy alloys (HEAs) developed by Yeh et al. since 2004 [1] have changed the traditional alloy design concept. An HEA is defined as an alloy consisting of 5 or more kinds of basic elements at equal molar ratios or near equimolar proportions, with an element radius difference of less than 15%, and with a content of each element between 5% and 35%. In addition, such multi-principal-element alloys form a simple solid solution and amorphous phase rather than a complex structure composed of many intermetallic compounds. These structural characteristics are ascribed to the high entropy effect and large lattice distortion as well as a sluggish diffusion effect [2]. Compared with traditional alloys, HEAs exhibit good combinations of strength and ductility [3], exceptional thermal stability [4], excellent hot hardness and softening resistance [5] and excellent resistance to corrosion [6] and wear [7], which makes them potential materials for applications requiring high temperature, strength and corrosion resistance.

To date, many kinds of processing routes have been used for preparing HEAs, such as arc melting [8–10], spark plasma sintering [11–14], mechanical alloying [15,16], plasma spray deposition [17], sputter deposition [18], and laser cladding [19–21]. Meanwhile, plenty of HEA systems have been developed. The alloying elements used most often in HEAs are Al, Co, Cr, Cu, Fe, Mn, Ni, and Ti. Based on these elements, HEAs such as AlCoCrFeNi [22,23], $AlCoCrFeNiTi_{0.5}$ [24], AlxCoCrCuFeNi [25], GdxCoCrCuFeNi [26] and CoCrFeNiZrx [27], have been developed. And also, AlxCoCrFeNi [28,29] represents a typical HEA and its microstructures and mechanical properties have been extensively investigated [22–25]. Although much of these literatures associated with the above materials have reported only solid solutions with simple crystal structures, such as face- or body-centered cubic structures (FCC and BCC respectively) and their related superlattice structures, it is expected that the microstructure of these alloys will still contain a variety of intermetallic compounds [1,30,31] and the HEAs may also contain minor elements that modify the properties of the base HEA [26,27]. Wang et al. [9] reported that, as the mole ratios of Al increase, the microstructures of AlxCoCrFeNi are transformed from the original single face-centered cubic (FCC) structure to a mixed structure of FCC and BCC structures, and finally to a single BCC structure, meanwhile, the hardness increases from 120 HV to 527 HV. However,

* Corresponding author.
E-mail address: cuihongzhi1965@163.com (H. Cui).

https://doi.org/10.1016/j.msea.2018.07.045
Received 21 March 2018; Received in revised form 11 July 2018; Accepted 12 July 2018

Table 1
Nominal composition of the $Al_XCrCo_{2-X}FeNi$ alloys.

Alloys	Nominal composition (at %)	Chemical composition (at%)					Mole ration of Al/Co
		Al	Cr	Co	Fe	Ni	
X = 1.0	AlCrCoFeNi	20	20	20	20	20	1:1
X = 1.2	$Al_{1.2}CrCo_{0.8}FeNi$	24	20	16	20	20	1.2:0.8
X = 1.4	$Al_{1.4}CrCo_{0.6}FeNi$	28	20	12	20	20	1.4:0.6
X = 1.6	$Al_{1.6}CrCo_{0.4}FeNi$	32	20	8	20	20	1.6:0.4

the cost of HEAs is much higher due to the addition of expensive elements on a large scale, such as Co, which is often the main reason for the limits in their applications.

To address this issue, here we study the effects of the mole ratios of Al:Co on the phases and microstructures of the $Al_XCrCo_{2-X}FeNi$ alloys. To date, research on the effect of the molar ratios of Al:Co on the microstructures and properties of HEAs has not been reported. In order to highlight the influence of Al and reduce the quantity of the added Co to minimize the costs under the maintaining good mechanical properties, the ratios of Al:Co were changed. Furthermore, the wear and compression characteristics of the $Al_XCrCo_{2-X}FeNi$ alloys were investigated.

2. Experiment

The samples were fabricated by spark plasma sintering in a vacuum. The elemental powders (purity higher than 99.95%) of Al, Cr, Co, Fe, and Ni were mixed thoroughly using a planetary ball mill. Four bulk alloys with nominal compositions (at%), namely AlCrCoFeNi, $Al_{1.2}CrCo_{0.8}FeNi$, $Al_{1.4}CrCo_{0.6}FeNi$ and $Al_{1.6}CrCo_{0.4}FeNi$, (Table 1) were spark plasma sintered in a vacuum and formed into a graphite die with 15-mm diameter using high-purity elemental constituents. The four kinds of powder samples were subsequently heated from room temperature to 1473 K at a heating rate of 100 K/min and then the samples were held at 1473 K for 15 min, followed by furnace cooling. During the sintering, a pressure of 32 MPa was maintained at both ends of the electrode. The size of the as-sintered HEAs cylindrical specimen was Φ 15 mmx10 mm.

The phases, compositions, microstructures, wear and fracture morphologies of the HEAs samples were characterized by X-ray diffraction (XRD), (Model D/Max 2500 PC Rigaku, Japan), scanning electron microscopy (SEM), (FEI-Nano Sem 450), electron probe microanalysis (EPMA), (JXA-8230, Japan), and transmission electron microscopy (TEM) respectively. The microhardness, wear behavior, and compressive behavior were tested using a microhardness instrument (FM-700/SVDM4R, Japan), a multifunctional abrasion testing machine (CETR-UMT-3MO, USA), a three-dimensional profilometer (Zeta-20, USA), and an electronic universal material testing machine respectively. The wear resistance is defined [7] as follows:

$$Wr = L/\Delta V$$

where W*r* is the wear coefficient, and △V is the volumetric loss of the specimen after sliding for a sliding distance L.

3. Results and discussion

3.1. XRD analysis

Fig. 1 shows the XRD of the SPS products with different molar ratios of Al:Co. At a molar ratio of Al:Co = 1:1, the phases in the product are composed of the FCC phase ($a_{FCC} \approx 3.59$ Å), the disordered BCC phase ($a_{\text{disordered BCC}} \approx 2.88$ Å), the ordered BCC phase ($a_{\text{ordered BCC}} \approx 2.88$ Å) and some σ phases. The diffraction peaks of the FCC structure have disappeared at a molar ratio of Al:Co = 1.2:0.8, and there are a disordered BCC phase, an ordered BCC phase, and a σ phase in the $Al_{1.2}CrCo_{0.8}FeNi$ alloy (Fig. 1). With a further increase in the mole ratio

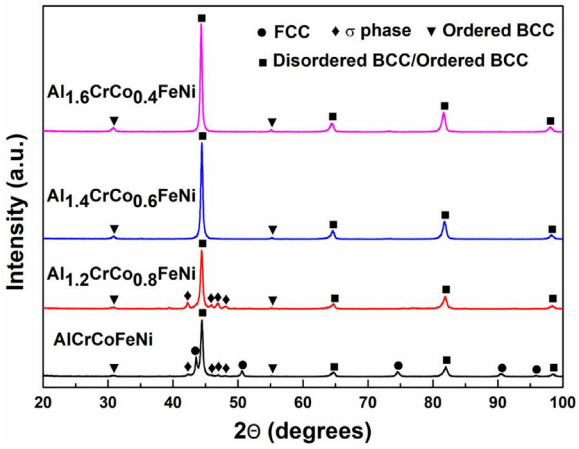

Fig. 1. XRD patterns of $Al_XCrCo_{2-X}FeNi$ alloys with various Al and Co contents.

of Al:Co, the diffraction peaks of the FCC phase and the σ phases disappeared. When Al:Co = 1.4:0.6 and 1.6:0.4, similar phases occur and they include a disordered BCC phase and an ordered BCC phase. It is apparent that, the relative intensity of the BCC reflection peak increases, and the diffraction peaks of the solid solution slightly shift to the left as the mole ratio of Al:Co increases, which might be attributed to the fact that Al possessed a relatively larger atomic radius (Fig. 1). The results show that the alloy elements dissolved in the solid solution lead to the lattice expansion.

3.2. Microstructure analysis

Fig. 2 shows the evolution of the microstructures with the increase the molar ratios of Al:Co. Fig. 2(a′), (b′), (c′), and (d′) correspond to the enlarged part of the red box in Fig. 2(a), (b), (c) and (d), respectively. As shown in Fig. 2(a) and (a′), the microstructures exhibit equiaxed grain structures. The element distribution of the different areas indicated by the arrow in Fig. 2 were measured by EDS and the results are shown in Table 2. In order to determine the distribution of the elements and phases, the EDS mapping of the $Al_XCrCo_{2-X}FeNi$ alloys is conducted, as shown in Fig. 3. It is evident that, the grain boundary is rich in Fe and Cr, and poor in Ni and Al, whereas the interior of grain is rich in Ni and Al. In addition, the interior of grain is composed of a periodic, fine-scale structure with bright and dark interconnected phases. The dark region is rich in Fe and Cr, and poor in Ni and Al, whereas the bright region is rich in Ni and Al, and poor in Fe and Cr. To further identify the phases and crystal structures of the phases, TEM is performed. The TEM bright-field images and diffraction patterns of the AlCrCoFeNi alloy are shown in Fig. 4. The chemical analysis of the different regions indicated by (b), (d), and (e) in Fig. 4 were measured by EDS and the results are shown in Table 3. Fig. 4(a) shows the TEM bright-field image and corresponding diffraction patterns in the grain boundary of the AlCrCoFeNi alloy, demonstrating that the Fe- and Cr-rich grain boundary belong to the FCC structure, which corresponds to ZA = $[\bar{1}12]_{FCC}$. In addition, the TEM bright-field image and corresponding diffraction patterns in the interior of grain are shown in Fig. 3(c). The results confirm that the interior of grain mainly consists of a matrix (rich in Ni and Al, bright region), and the precipitates (rich in Fe and Cr, dark region). Based on the calibration of the diffraction patterns of the matrix and the precipitates, the crystal structure of the matrix is an ordered BCC structure, and the precipitates exhibit a disordered BCC structure, which corresponds to the same ZA = $[001]_{BCC}$, as shown in Figs. 3(d) and 3(e). As shown in Fig. 1, the σ phases are identified by XRD at molar ratios of Al:Co = 1:1 and Al:Co = 1.2:0.8, respectively. Fig. 5 shows the TEM bright-field images and corresponding diffraction patterns of the AlCrCoFeNi and $Al_{1.2}CrCo_{0.8}FeNi$ alloy, respectively. From Fig. 5(a), it appears that the σ phase forms in the boundaries in typical strip shape,